2007

# Large-Scale Numerical Modeling of Melt and Solution Crystal Growth

Jeffrey J. Derby
*University of Minnesota - Twin Cities*

James R. Chelikowsky
*University of Texas at Austin*

Talid Sinno
*University of Pennsylvania*, talid@seas.upenn.edu

Bing Dai
*University of Minnesota - Twin Cities*

Yong-Il Kwon
*University of Minnesota - Twin Cities*

***See next page for additional authors***



J.J. Derby *et al.* Large-Scale Numerical Modeling of Melt and Solution Crystal Growth. In Perspectives on Inorganic, Organic, and Biological Crystal Growth: From Fundamentals to Applications, 13th International Summer School on Crystal Growth Eds. M. Skowronski, J. J. DeYoreo, and C. A. Wang. (2007).

# Large-Scale Numerical Modeling of Melt and Solution Crystal Growth

**Abstract**
We present an overview of mathematical models and their large-scale numerical solution for simulating different phenomena and scales in melt and solution crystal growth. Samples of both classical analyses and state-of-the-art computations are presented. It is argued that the fundamental multi-scale nature of crystal growth precludes any one approach for modeling, rather successful crystal growth modeling relies on an artful blend of rigor and practicality.

**Keywords**
Continuum transport, heat transfer, fluid mechanics, atomistic models, defect dynamics, segregation, morphological instability, solidification

**Disciplines**
Chemical Engineering | Engineering

**Comments**
J.J. Derby *et al.* Large-Scale Numerical Modeling of Melt and Solution Crystal Growth. In Perspectives on Inorganic, Organic, and Biological Crystal Growth: From Fundamentals to Applications, 13th International Summer School on Crystal Growth Eds. M. Skowronski, J. J. DeYoreo, and C. A. Wang. (2007).



**Author(s)**
Jeffrey J. Derby, James R. Chelikowsky, Talid Sinno, Bing Dai, Yong-Il Kwon, Lisa Lun, Arun Pandy, and Andrew Yeckel

# Large-Scale Numerical Modeling of Melt and Solution Crystal Growth

Jeffrey J. Derby*, James R. Chelikowsky†, Talid Sinno**, Bing Dai*, Yong-Il Kwon*, Lisa Lun*, Arun Pandy* and Andrew Yeckel*

*Department of Chemical Engineering & Materials Science and Minnesota Supercomputing Institute, University of Minnesota, Minneapolis, MN 55455, USA
†Institute for Computational Engineering and Science, University of Texas at Austin, Austin, TX 78712, USA
**Chemical and Biomolecular Engineering, University of Pennsylvania, Philadelphia, PA 19104, USA

**Abstract.** We present an overview of mathematical models and their large-scale numerical solution for simulating different phenomena and scales in melt and solution crystal growth. Samples of both classical analyses and state-of-the-art computations are presented. It is argued that the fundamental multi-scale nature of crystal growth precludes any one approach for modeling, rather successful crystal growth modeling relies on an artful blend of rigor and practicality.

**Keywords:** Continuum transport, heat transfer, fluid mechanics, atomistic models, defect dynamics, segregation, morphological instability, solidification
**PACS:** 02.60.Cb, 81.10.-h, 81.10.Aj, 81.10.Dn, 81.10.Fq

## INTRODUCTION

Processes developed to grow large, single crystals from liquid phases are among the most challenging and precise in engineering practice, and large-scale, numerical modeling has been vital to advance crystal growth production technology to current levels. However, there are other good reasons to model crystal growth. At a basic level of scientific inquiry, models make use of the most precise language ever invented by mankind, namely mathematics, to enable the disciplined application of reason and analysis toward the goal of understanding the fundamentals of crystal growth. Modeling also proves useful to unravel the simultaneous interaction of many nonlinear phenomena that occur during crystal growth toward the goal of process improvement and optimization. Finally, a mathematical model provides a solid framework to be employed toward the goal of improved design and control of crystal growth processes.

The paradigm of modeling is to build an appropriate mathematical representation of a system, solve its underlying equations, typically by numerical methods, and creatively apply the model toward a set of well-defined questions. Toward the ultimate goal of using a model to answer questions, it is extremely important that the model be validated and verified [1]. Verification addresses the question of whether a computer code is accurately solving the mathematical equations posed by the model. Validation addresses the question of whether the mathematical model is faithfully representing the behavior of the system via the comparison of model predictions to experimental measurements.

CP916, *Perspectives on Inorganic, Organic, and Biological Crystal Growth: From Fundamentals to Applications, 13th International Summer School on Crystal Growth*
edited by M. Skowronski, J. J. DeYoreo, and C. A. Wang

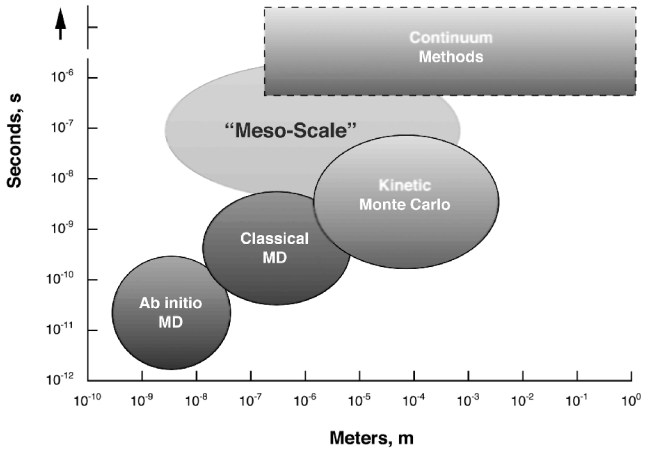


**FIGURE 1.** Different modeling approaches are appropriate for various length and time scales. Typical sizes of features from bulk melt and solution growth span from nanometers to meters.

However, validation should not be the overriding goal of modeling. Indeed, it has been stated that [2], "The purpose of models is not to fit the data but to sharpen the questions."

The physics of crystal growth encompasses a wide variety of phenomena that occur over a vast spectrum of length and time scales, literally ranging from atoms to cubic centimeters of material. Consider the following: the unit cell of most inorganic crystals is on the order of 1–10 nanometers; growing interfaces may include surface features, such as terraces, which range in size from from 0.1–1 microns; defects in crystals can range from atomic dimensions for point defects to 10 microns or larger for second-phase inclusions; step bunches in solution growth can be as large as 100 microns; and the dimensions of the desired bulk crystal can range from centimeters to meters in size. Unfortunately, one cannot pose and solve a mathematical model for crystal growth completely from first-principles due to these disparate scales. Instead, many different approaches and tools are applied to model different aspects of crystal growth, as depicted in Figure 1.

At a microscopic scale of tens of nanometers or less, *ab initio* molecular dynamics methods can be employed to study atomic behavior. Unfortunately, while quite rigorous in their approach, even using today's fastest computers these methods are too computationally expensive to be applied to systems of more than a few thousand atoms or for describing times scales of greater than hundreds of picoseconds. Molecular dynamics methods based on classical potentials can compute for much larger ensembles and longer time scales. To model atomistic behavior at even larger length scales and longer time scales, kinetic Monte Carlo methods have been developed. More details will be provided about these methods later in this paper.

On a macroscopic scale, continuum methods are gainfully applied; examples of these models will also be discussed. Significantly, there are many important phenomena associated with crystal growth that occur on a "meso-scale" comprising hundreds of

nanometer to tens of microns and occurring over long times scales (e.g., microseconds or longer). These phenomena are difficult to model by atomistic methods, due to the long time scales involved, and challenging for continuum methods, due to the very small length scales. Such phenomena require innovative, "multi-scale" approaches, which, despite much fanfare, are still at nascent stages of development.

This challenge of scales motivates the need to formulate crystal growth models that include enough physics to make realistic, usable predictions, yet that are simple enough to remain tractable with today's computational capabilities. In the case of bulk crystal growth, the greatest purpose that modeling can serve is to directly connect processing conditions to final outcomes. Since bulk crystals usually are incorporated into electronic, optical, or optoelectronic devices, final outcome is most often measured in terms of the crystal properties relevant to these devices. These crystal properties are in turn determined by the chemical composition and structure of the crystal, particularly the types and distributions of various crystalline defects. For the crystal growth modeler, the ultimate task is to connect processing conditions to the morphology, chemical composition, and defect structure of the crystal.

## CRYSTAL GROWTH MODELING

Crystal growth modeling involves the construction of a mathematical description of a crystal growth system, the solution of the governing equations of the model, and the interpretation of the modeling results. Below, brief discussions of governing equations and solution techniques are presented for modeling crystal growth at different scales.

### Continuum transport

Continuum transport modeling is the most highly developed aspect of crystal growth modeling and much has already been written on the subject. The seminal treatise on the general subject of continuum transport phenomena is the textbook of Bird, Stewart, and Lightfoot [3]. At least one book devoted to modeling of transport phenomena specific to crystal growth has been published [4], featuring chapters by different authors writing on various topics. A number of chapters on the subject can be found within other works, including a general introduction to the subject by Derby [5], an extensive review of convection in melt growth by Müller and Ostrogorsky [6], and some more recent accounts of specific topics in crystal growth modeling [7–13]. Although fifteen years old now, the review article by Brown [14] remains remarkably current in many respects and is essential reading for anyone contemplating modeling. Of particular note are the proceedings of the series of International Workshops on Modeling in Crystal Growth [15–18]. These workshops have been immensely successful at bringing together leading crystal growth modelers from around the world, and their proceedings provide an indispensable resource for tracking the state of developments in modeling of bulk crystal growth.

The transport of heat, mass, and momentum is especially important in bulk crystal growth processes. Governing equations are written to describe the conservation of these

quantities within the solid crystal and the accompanying fluid phase. A brief accounting of these phenomena and their governing equations is given below.

Flow in the fluid phase is especially important for the transport of heat and mass via convection in bulk crystal growth systems. For liquids, such a the molten phase in melt growth or the solution phase in solution growth, flows are described by conservation equations written for momentum and continuity of an incompressible, Newtonian fluid with the application of the Boussinesq approximation to describe fluid density changes:

$$\rho\left(\frac{\partial \mathbf{v}}{\partial t}+\mathbf{v}\cdot\nabla\mathbf{v}\right)=-\nabla p+\mu\nabla^2\mathbf{v}+\rho_0\mathbf{g}[1-\beta_T(T-T_0)-\beta_s(c-c_0)]+\mathbf{F}(\mathbf{v},\mathbf{x},t), \quad (1)$$

where $\rho$ is the density of the fluid, $\mathbf{v}$ is the velocity field, $t$ is time, $\nabla$ is the gradient operator, $p$ is the pressure field, $\mu$ is the fluid viscosity, $\mathbf{g}$ is the gravitational vector, $\beta_T$ and $\beta_s$ are the thermal and solutal expansivities, respectively, $T$ is temperature, $c$ is concentration, the subscript zero denotes the reference state about which the linear dependence of the density is approximated, and $\mathbf{F}(\mathbf{v},\mathbf{x},t)$ is an additional body force, e.g., that which results from the application of a magnetic field to a conducting fluid. The requirement for continuity of the fluid phase takes on the following form:

$$\nabla\cdot\mathbf{v}=0, \quad (2)$$

which states the divergence of the velocity field must be everywhere zero. Collectively, these two expressions constitute the celebrated *Navier–Stokes* equations.

Flows driven by buoyancy, referred to as *natural convection*, are important in all bulk crystal growth systems due to thermal or solutal gradients. In addition, temperature or compositional gradients along a liquid-gas interface can drive very strong flows arising from the variation of surface tension along the surface. Often referred to as *Marangoni* flows, these are important in many meniscus-defined melt growth systems, such as the Czochralski and floating zone methods. *Forced convection* flows are driven by applied rotation of crystal or crucible or, in solution growth systems, by pumping or stirring mechanisms. Also of great importance in many bulk growth systems are time-dependent or turbulent flows, which arise naturally if the driving forces are strong enough. These flows dramatically affect the nature of continuum transport to the crystal interface. The application of strong stationary or rotating magnetic fields has been applied to electrically-conductive melts in attempts to control such flows.

The transport of heat and mass can be determined from solution of the appropriate governing equations. The energy balance equation is given by the following expression:

$$\rho C_p\frac{\partial T}{\partial t}+\rho C_p\mathbf{v}\cdot\nabla T=\kappa\nabla^2 T, \quad (3)$$

where $C_p$ is the heat capacity and $\kappa$ is the thermal conductivity of the fluid. For media which possess some transparency to infrared radiation, the transport of energy via internal radiative transport may also be important in high-temperature crystal growth systems, and an extra term must be added to the above equation [19]. The exchange of thermal radiation among surfaces is also very important in many high-temperature growth systems. These radiative processes are described by terms which are strongly

nonlinear in temperature, thus posing significant modeling challenges. Heat transfer is also very strongly influenced by thermal boundary conditions, i.e., the conditions imposed on the crystal and fluid by the system design. The modeling of heat transfer in high-temperature melt growth furnaces is itself a significant technical challenge due to complicated geometries and radiation heat transfer.

The conservation equation for a dilute species in a fluid is given by:

$$\frac{\partial c}{\partial t} + \mathbf{v} \cdot \nabla c = \mathscr{D} \nabla^2 c, \tag{4}$$

where $\mathscr{D}$ is the diffusion coefficient of the species. Mass transfer in bulk crystal growth systems is largely determined by the interactions of diffusion and convection near the liquid-crystal interface. At a growing crystal surface, the equilibrium partitioning of a solute between solid and fluid phases coupled with diffusion and convection results in segregation, i.e., the inhomogeneous distribution of a solute in a grown crystal. These phenomena are discussed in more detail in ensuing sections.

## The crystal interface

The manner in which the crystal interface is represented is a central feature of bulk crystal growth models. A self-consistent growth model requires that the interface geometry be computed as part of the solution to the transport problem, i.e., as a free or moving boundary. For the case of melt growth, a mathematical expression of the normal growth velocity of the interface, $V_g$ is given by

$$V_g = \beta \Delta T, \tag{5}$$

where $\beta$ denotes a kinetic coefficient and $\Delta T$ is the driving force for crystallization,

$$\Delta T = T_i - T_m \left(1 - \frac{\gamma}{L} \mathscr{H}\right) \tag{6}$$

where $T_i$ represents the interface temperature, $T_m$ is the melting temperature of a planar interface , $\gamma$ is a capillary coefficient, $L$, is the latent heat of solidification, and $\mathscr{H}$ depicts the local mean curvature of the interface. For an atomically rough interface, the kinetic coefficient becomes large enough so that the undercooling $\Delta T$ goes to zero and $T_i = T_m(1 - \gamma \mathscr{H}/L)$. Here, the rate of interface movement is controlled by the flow of latent heat away from the interface. In many bulk melt-growth systems, the interface is flat enough so that capillarity is unimportant, and the interface is located along the melting point isotherm of the system, $T_i = T_m$.

From an algorithmic point of view, two methods are primarily employed for computing the location of the crystal interface. Front-tracking methods define a discrete moving surface to separate the interface between crystal and melt, and diffuse-interface methods treat the interface as a region of finite thickness across which physical properties vary rapidly but continuously from one bulk value to the other. Both methods have been used with great success to model different crystal growth problems. Front-tracking methods,

such as the *isotherm method* [20], have an advantage in accuracy and numerical efficiency, but their implementation becomes problematic when the shape of the interface becomes complicated, e.g., as in representing the shape of a dendrite. Diffuse-interface methods, such as the *phase field method* [21, 22], come to the fore in such situations; they are able to compute interface shapes of great complexity, albeit at a higher computational cost for a given level of accuracy.

Modeling the growth velocity of a crystalline surface in bulk solution growth is much more problematic than in melt growth systems, since interfacial kinetics are much more important. The simplest representation of interface velocity and growth is

$$V_g = \beta_k \sigma, \tag{7}$$

where $\beta_k$ denotes a kinetic coefficient and $\sigma$ is the supersaturation. The supersaturation is defined as $\sigma \equiv \Delta\mu_g / k_B T = \ln(C/C_e)$, where $\Delta\mu_g$ is the change in the chemical potential between the crystal and liquid, $k_B$ is the Boltzmann constant, and $C$ and $C_e$ are the actual and equilibrium molar concentrations. The kinetic coefficient in this expression varies strongly as a function of the detailed nature of the surface, posing great challenges for realistic modeling. Indeed, predicting the shape of crystals growing from the solution phase is still a formidable undertaking [23–25].

## Defect dynamics models

Modeling has been gainfully employed to understand the origins of several types of defects in bulk crystals grown from the melt and to optimize growth conditions to reduce their numbers. During the growth of semiconductor crystals, a large number of dislocations can be produced via dislocation formation and multiplication processes driven by thermal stresses generated during growth and cooling. While the necking process developed by Dash for Czochralski growth has allowed large elemental semiconductor crystals (e.g., silicon and germanium) to be grown dislocation-free, large compound semiconductor crystals, such as gallium arsenide and cadmium telluride, are plagued by high levels of dislocations. Modeling heat transfer in growth systems has been successfully employed to minimize thermal stresses and dramatically reduce defect densities of bulk compound semiconductor crystals. Völkl [26] and Miyazaki [27] provide extensive reviews of this area.

Intrinsic point defects also arise naturally during the growth of all bulk crystals, and their fate under growth conditions determines the properties of the resultant material. Such point defects arise from their entropic contribution to lowering the Gibbs energy of the crystal, which varies exponentially with temperature, and these defects also diffuse through the lattice via processes which are strongly thermally activated. There has been much recent progress in understanding how point defects arise, move, and interact in silicon to produce micro-defects, such as voids arising from the condensation of excess vacancies and networks of dislocation loops formed by excess interstitials. Accurate modeling is required to predict these effects and optimize growth conditions. Such efforts have been referred to as *defect engineering*. A brief overview is presented below based on the overview of Sinno *et al.* [28].

Defect dynamics models aim to connect the dynamics of point defect dynamics and microstructural evolution with processing conditions present during crystal growth. These models have been extremely successful at describing the size distribution evolution of defect aggregates in silicon crystal growth and wafer processing at a scale that allows for direct comparison to experimental measurements. For example, the industrial use of defect dynamics models for predicting the size distribution of voids formed by vacancy aggregation in single-crystal silicon is now widespread [28, 29]. More recently, these models have been extended to include multicomponent interactions between vacancies and oxygen so that the formation of complex defects such as oxide precipitates can be predicted. The latter are a critical component of wafer engineering for advanced microelectronic device fabrication.

Mathematical models for defect dynamics are developed in terms of microscopic transport theory involving equilibrium, diffusion, convection, and reaction of defect species created by combinations of vacancies, interstitials, and impurities. Consider either a single point defect species undergoing aggregation (e.g., a vacancy or interstitial) within a crystalline matrix. The conservation equation for this species can be written in terms of the molar concentration of that species, $c_1$, as,

$$\frac{Dc_1}{Dt} = \nabla \cdot [\mathscr{D}_1(T)\nabla c_1] - \sum_x k_x c_1 c_x - \frac{\partial}{\partial t}\int_2^\infty n f(n,\bar{r})dn, \tag{8}$$

where the substantial derivative, $D/Dt \equiv \partial/\partial t + V\partial/\partial z$, is defined as the rate of change of concentration at a point moving with the velocity, $V$, of the growing crystal (which is moving in the $z$-coordinate direction. The second term represents the reaction network coupling this species and others (denoted by the subscript $x$) in the system. The last term in eq. (8) represents the incorporation of monomers into clusters of all possible sizes. Here, is the concentration of clusters of point defect $x$, and size $n$ at a given position, $\bar{r}$, within the crystal.

Balance equations for smaller clusters are developed using individual Master Equations for each aggregate size and are written as,

$$\frac{Dc_n}{Dt} = J_n - J_{n+1}, \tag{9}$$

where $J_n$ is the nucleation flux, given by

$$J_n = g(n-1)c_{n-1} - d(n)c_n, \tag{10}$$

and $c_n$ represents the concentration of clusters of size $n$. The functions $g(n)$ and $d(n)$ represent the growth and dissolution rates for clusters of size $n$, respectively, and are determined from from atomistic simulations, as will be discussed below.

Large clusters contain a very large number of monomers and cannot be described feasibly with the Master Equations (9). A common approach is to use an approximation in which the majority of the Master Equation sequence is reduced into a single Fokker-Planck equation by assuming that the cluster size can be represented continuously [30]; the Fokker-Planck equation is then matched to the Master equation sequence at some

given cluster size. The Fokker-Planck equation is generally given by,

$$\frac{Df}{Dt} = \frac{\partial}{\partial n}\left(A(n)f - B(n)\frac{\partial f}{\partial n}\right), \tag{11}$$

where

$$A(n) = g(n) - d(n) - \frac{\partial B(n)}{\partial n}, \tag{12}$$

and

$$B(n) = \frac{1}{2}[g(n) + d(n)]. \tag{13}$$

It is important to realize that the above equations cannot stand alone to produce meaningful results. The microscopic phenomenological parameters in eq. (8) and the functions $g(n)$ and $d(n)$ in eq. (10) are not known in general and are not measurable by any direct experimental means. Therefore, the only source for these functions is via atomistic simulations capable of realistic predictions. These simulations represent one of the multi-scale links needed for the defect dynamics analysis and are discussed in the section immediately following. Next, input is needed from a global heat transfer model to compute the temperature profile throughout the growing crystal. The accuracy of the heat transport model is also extremely important because of the Arrhenius temperature dependence of most of the thermodynamic and transport properties. Thus an accurate global model of the crystal growth process is another multi-scale input that is required to model defect dynamics.

## Atomistic simulation

Modern atomistic simulation techniques, such as molecular dynamics and kinetic Monte Carlo methods, are being applied to model features of crystal growth systems. These techniques are showing great promise for a obtaining deeper understanding of crystal growth; however, they are typically restricted to describing systems characterized by very small length scales over very short time scales. Jackson [31, 32], Gilmer [33], Van der Eerden [34], and Sinno [35] provide good overviews.

The heart of atomistic analyses is computing the motion of individual atoms in a system, a technique known as *molecular dynamics*. The trajectory of each atom is computed from an appropriate intial condition and by considering the interatomic forces among all entities. Methods which employ quantum mechanical forces (obtained by approximate solutions to the Schrödinger equation) are refereed to as *ab intio* simulations. Since they are derived from a rigorous representation of atomic interactions, they can be extremely accurate but are also very expensive to compute. Faster computation is achieved by replacing the quantum forces by those computed from a relatively simple representation of the interatomic potential. Such methods are often refereed to as *classical* or *empirical* molecular dynamics simulations. While not as rigorous as ab initio methods, classical techniques have been used successfully to carry out very large-scale computations and yield realistic results. The fastest class of atomistic simulation substitute for the integration of the equations of motion (as is done in molecular dynamics) with hops of atoms

on a pre-defined lattice, with each hop computed as a probabilistic event weighted by an associated transition energy and corresponding to specified time horizon. Due to the elements of chance involved with each step in time, such techniques are referred to as *Kinetic Monte Carlo* models.

## SAMPLES OF CRYSTAL GROWTH ANALYSIS

As previously emphasized, bulk crystal growth is characterized by strongly interacting and often very nonlinear phenomena. Theory and modeling has allowed many of these behaviors to be analyzed and more completely understood; a few examples, some classical, some state-of-the-art, are discussed below.

### Atomistic simulation of II–VI melts

Compound II–VI semiconductors, such as cadmium telluride and its alloy cadmium zinc telluride, pose formidable challenges for melt crystal growth [36–38]. Some of these challenges arise from the behavior of the molten, or liquid, state of II–VI compounds, which is poorly understood. Indeed, the behavior of liquid II–VI materials is far different from more classical semiconductors. For example, Glazov *et al.* [39] observed that changes in various properties upon melting of CdTe were consistent with much less disassociation than other semiconductors and thus a significant amount of ordered melt structure. From electrical conductivity measurements, they further postulated that the melting of CdTe is a solid semiconductor–liquid semiconductor transition rather than the semiconductor–metal transition associated with group IV and III–V materials. Glazov *et al.* [39] also hypothesized that atomic chains of Te are an essential feature of liquid CdTe. Cystal growth folklore is replete with references to the beneficial effect of superheating the melt on CdTe crystal growth [36, 40]. The notion is that superheating the melt breaks up its structure, thereby more readily allowing the phase change from liquid to solid to occur. As a final piece of evidence consistent with this scenario, recently Feychuk *et al.* [41] observed temperature oscillations via differential thermal analysis while holding CdTe melt at certain temperatures. They claimed that such melt temperature oscillations coincide with endothermic effects that can only be caused by melt structural transformations.

*Ab initio* molecular dynamics simulations by Chelikowsky and colleagues [42–47] revealed a rich set of physical behaviors for II–VI liquids. A snap-shot showing a supercell with typical liquid microstructure at one of the time steps of a molecular dynamics simulation of CdTe just above its melting point is shown in Figure 2(a). Godlevsky *et al.* [42] showed conclusively that the CdTe does behave as a liquid semiconductor. This and subsequent studies also demonstrated the existence of tellurium chain structures in the melts of CdTe and ZnTe. This is illustrated in Figure 2(b), where atoms of Te are shown in the supercell geometry of a calculation of liquid CdTe near its melting point. There are Te filaments reaching the length of the supercell. Because of the imposed periodicity of the system, some of the Te chains terminating at the opposite sides of the supercell

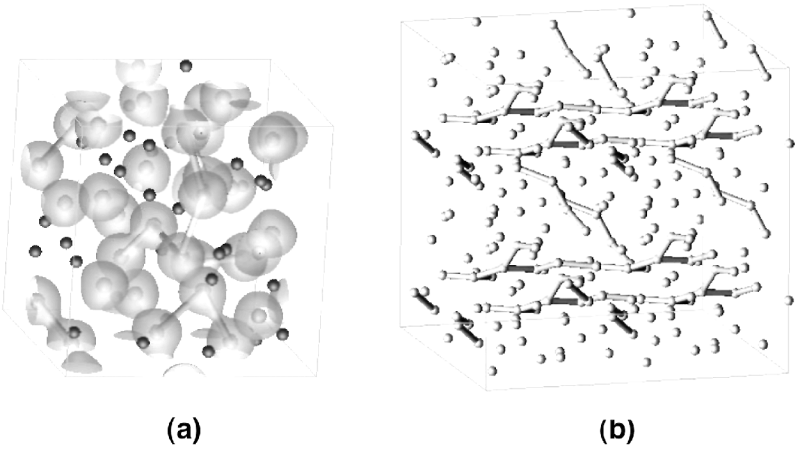


**FIGURE 2.** (a) Typical liquid microstructure at one of the time steps of a molecular dynamics simulation of CdTe just above its melting point. Dark atoms correspond to Cd; light atoms correspond to Te. A charge density surface is shown for the value of half of the maximum. (b) Ab initio simulations predict long, helical chains of tellurium in liquid CdTe near the melting-point temperature. The computational supercell is shown here with only atoms of Te and bonds between them displayed.

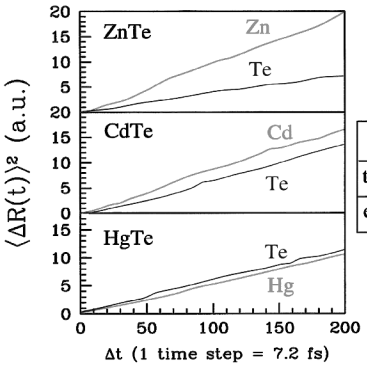


$$D = \frac{\langle R(t) \rangle^2}{6t}$$

$D\ (10^5\ cm^2\ s^{-1})$

| | Cd | Te |
|---|---|---|
| theory | 6.7 | 5.2 |
| exp | — | 5.0 |

**FIGURE 3.** The time dependence of the mean square displacement of atoms in liquid II–VI compounds. The simulation temperature is near that of the melting point. The mean squared displacements are in atomic units and the time is given in simulation steps.

become "infinite." This is an important structural observation; on a longer time scale, such chains may interfere with the phase change at a liquid-solid interface.

In addition to structural issues, these ab inito models can be applied to examine kinetic issues. By following the atomic positions in the liquid state as a function of time, we can calculate the self-diffusion of the constituent species in the melt [46]. The diffusion

constant can be determined from

$$D = lim_{t\to\infty} \frac{< [R(t)]^2 >}{6t}. \tag{14}$$

One can plot the squared displacement, $R^2$, averaged over the species of interest as a function of time; the slope of this curve will yield the diffusion constant. In Figure 3, we illustrate the displacement versus time for three different II–VI compounds. Although our ensemble only contains 64 atoms, the statistics are adequate to give reliable diffusion constants. An experimental value for the diffusion of Te in liquid CdTe is available [37], namely $D$(Te) = 5.0 $\times$ $10^{-5}$ cm$^2$/sec. Our theoretical value is $D$(Te) = 5.2 $\times$ $10^{-5}$ cm$^2$/sec. This value corresponds to a temperature near the melting point. The computed values for the self-diffusion coefficient of the other atoms correlate with atomic wieght, with more massive species diffusing more slowly. We note that other methods such as tight binding molecular dynamics or classical molecular dynamics which have been performed for IV and III-V semiconductors typically underestimate the diffusion constant by a factor of two [46].

## Step models for solution crystal growth

Under typical situations in solution growth where the interface is at a temperature below the roughening transition, the surface morphology which minimizes the free energy is an atomically smooth plane associated with the underlying crystalline structure, referred to as a *singular* face or facet. The rate of growth of the crystal is then determined by how fast new layers can be added. However, if two-dimensional nucleation must occur to start a new layer on a singular surface, the rate of crystallization would be implausibly low compared to actual observations. Burton and Cabrera [48] postulated that a *vicinal* surface, i.e., an orientation in the *vicinity* of a facet plane, would contain enough steps to rectify this large discrepancy between theory and observation. Namely, the slow rate of step nucleation could be circumvented if the layers were already present on the surface. At the same time, Frank [49] noted that dislocations are present in nearly all crystals and that a screw dislocation intersecting a face would act as a continuous source of steps. *Burton–Cabrera–Frank,* or BCF, theory [50] describes the growth of singular crystal faces as a mechanism of step generation and movement.

There is a vast literature devoted to modern experimental and theoretical studies of step growth mechanisms; see the reviews Jeong and Williams [54] and Krug [55, 56]. That steps even exist is a curious feature of the nature of crystals. Steps on a vicinal surface are atomic features, one unit cell in height, that separate individual lattice planes. These steps are separated by terraces, each of which is an atomically flat, singular surface. As explained by Krug [55], the cost in terms of free energy to form a new step segment is large enough to render these steps thermodynamically stable at sufficiently low temperatures. These long-lived surface features makes them suitable as a basis to construct *mesoscopic* models that describe the evolution of surface morphology via the representation of atomic-size steps embedded within in a continuum description of mass transport.

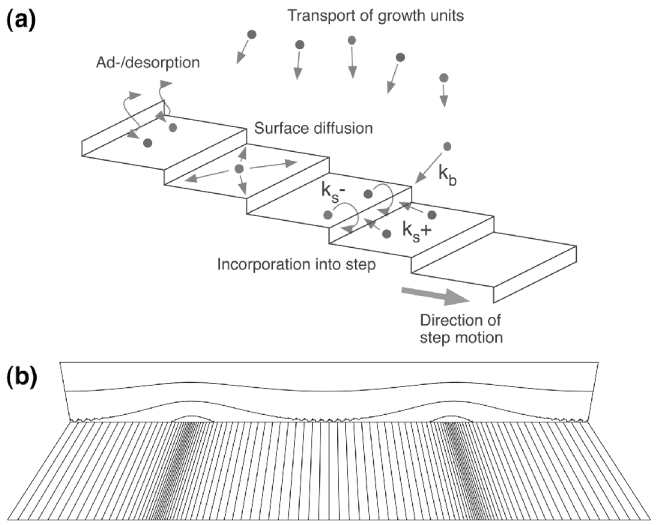


**FIGURE 4.** (a) A depiction of the mechanisms responsible for the growth of a vicinal crystalline surface from a liquid solution. (b) Two step bunches are indicated by the closely spaced lines on the crystal surface; contours of bulk supersaturation are shown above the surface, with lowest supersaturation values immediately above the step bunches [65].

The BCF mechanism of steps moving along a crystalline surface is firmly established, yet this picture is not enough to explain the growth of crystals from liquids. Since the diffusion of solute molecules through a liquid phase is quite slow, there are nearly always significant mass transfer effects on growth. A schematic depiction of the transport of species to the surface steps followed by their subsequent incorporation, causing step movement is shown in Figure 4(a). Such effects are known to slow the overall rate of growth of the crystal and, under certain circumstances, can lead to morphological instabilities during growth. Chernov [51], Gilmer, Ghez, and Cabrera [52],and Van der Eerden [53] put forth analytical models to account for additional incorporation and transport effects in significant advances to the basic BCF model.

Of particular interest are step bunching instabilities which drive otherwise parallel, equidistant steps to form bunches, i.e., features where many closely spaced steps are separated by regions with relatively few, widely spaced steps. Chernov *et al.* [57–60] performed an impressive series of rigorous linear stability analyses of a vicinal surface with respect to harmonic perturbations of the step strain. Their analyses showed that the coupling of kinetic anisotropy, resulting from the variation of step distribution on the crystal surface, with convective solute transport above the steps lead to an instability for the case of strong fluid flows in the same direction as the step motion, in agreement with experimental observations [61].

We have developed a mesoscopic, step-growth model [62, 63] and have performed transient simulations of perturbed step trains under solution flow, confirming that and such flows can drive the formation of large step bunches [64, 65]. While the discrete

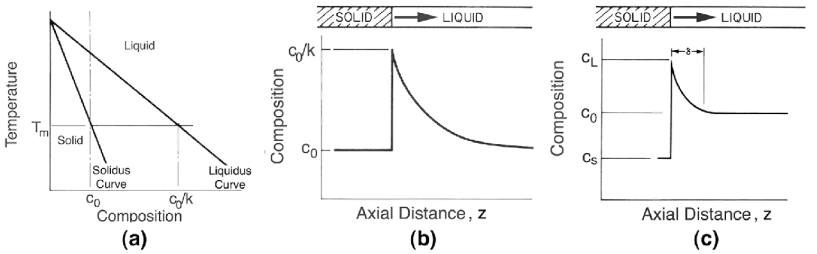


**FIGURE 5.** The solidification of a dilute binary alloy: (a) simplified phase diagram, (b) diffusion-limited axial segregation, and (c) axial segregation as depicted by the BPS model.

description of steps used in our step growth model is different from the continuum description in Chernov's linear stability analyses, good agreement was shown for steps in direct incorporation mode under a similar set of growth conditions. One of the bunched states computed by our model is shown in Figure 4(b), where two step bunches are shown as closely spaced lines that represent straight, parallel steps on the crystal surface .Bulk supersaturation contours above the steps show depletion regions around these step bunches. A sufficiently strong flow in the same direction as the step motion, both from left to right in the figure, causes the formation of step bunches.

## Segregation in directional solidifcation

For a dilute species (often called a *dopant*) added to a pure material, the phase behavior of the nearly-pure material can be described by a phase diagram of temperature plotted as a function of concentration (at constant pressure), as shown in Figure 5(a). The important behaviors, from the point of view of crystal growth, are that the solid in equilibrium with the liquid at a fixed temperature differ in composition and that the equilibrium melting (or freezing) temperature is a function of composition. The first of these phenomena gives rise to *segregation,* referring to the partitioning of a dopant between the solid and melt which results in a crystal of inhomogeneous composition, even when grown from an initially uniform-composition melt. The second phenomenon, when coupled with segregation during growth, is responsible for the morphological instability known as *constitutional supercooling* and will be discussed in the next section.

Classic explanations of dopant segregation [66] involve directional solidification, where a crystal is growing into a melt in one direction and both phases initially have the same solute composition, $c_0$. For the case of no melt mixing and a partition coefficient, $k$, less than unity, dopant is rejected from the growing crystal and diffuses away from it. This flux causes the the melt dopant concentration at the interface to increase in time, until it is exactly $c_0/k$, as depicted schematically in Figure 5(b). Under these conditions, axial segregation is said to be *diffusion-limited* and, barring initial and final transients, gives rise to a constant composition $c_0$ along the length of the crystal. Tiller *et al.* [67, 68] were the first to lay out the quantitative details of axial dopant segregation in a crystal growing under purely diffusive conditions.

Convection in the melt disrupts this appealing diffusion-controlled scenario by altering the form of the concentration profile in the melt. The *BPS model* of Burton, Prim, and Schlicter [69] postulates a stagnant film in front of the interface of thickness $\delta$. Transport is assumed to occur only by diffusion within the film and by perfect convective mixing beyond the film, leading to the dopant concentration profile depicted in Figure 5(c). Under this scenario, the axial distribution of a dopant in the crystal is given by

$$\frac{c_s}{c_0} = k_{\text{eff}}(1-f)^{(k_{\text{eff}}-1)}, \tag{15}$$

where $c_s$ is the concentration of dopant in the crystal, $c_0$ is the initial concentration of solute in the bulk, $f$ is the fraction of melt solidified, and $k_{\text{eff}}$ is an "effective" distribution coefficient given by

$$k_{\text{eff}} = \frac{k}{k+(1-k)\exp(-V_g\delta/\mathscr{D})}, \tag{16}$$

where $k$ is the equilibrium distribution coefficient, $V_g$ is the growth velocity of the crystal, and $\mathscr{D}$ is the diffusion coefficient of the dopant in the melt. If $\delta \to \infty$, the effective segregation coefficient approaches unity, and the constant axial concentration profile for diffusion-controlled growth is obtained. As $\delta \to 0$, complete mixing of the melt is implied, $k_{\text{eff}} \to k$, and the *Scheil equation* [70] for axial segregation is recovered. The BPS model is often very effective for fitting experimental segregation data by suitable choice of the parameter $\delta$.

The simplicity and elegance of the BPS expression is perhaps a bit misleading, since it has virtually no predictive capabilities. The underlying idea for this model is too simple; there is no precise physical meaning of the parameter $\delta$, since flows in real systems are never completely stagnant nor intense enough to produce perfect mixing. In addition, segregation *across* the face of the crystal can be more important than segregation along its length, and this effect is ignored in the one-dimensional solidification model discussed above. Shortcomings of the stagnant layer concept and similar boundary layer models have been discussed by Wilcox [71] and Rosenberger and Müller [72]. Brown and Kim [73] provided an erudite discussion of the validity of the stagnant layer model by comparison with results from detailed numerical simulations of Bridgman growth.

## Morphological instability in directional solidification

The one-dimensional directional solidification model presented above can be used to understand the *morphological stability* of a crystal interface during growth. The situation leading to instability is depicted in the top, right plot of Figure 6. An axial temperature gradient is applied to the system to maintain growth, with the interface at $T_C$ and the temperature rising as it extends into the melt (shown by the dashed line). Typically, thermal diffusion processes are much faster than mass diffusion, so the temperature profile is linear over the length scale characteristic of the dopant diffusion layer in front of the solidification interface. Also shown in this plot is a curve that denotes the equilibrium freezing temperature of the melt, or the liquidus temperature, $T_L$, in

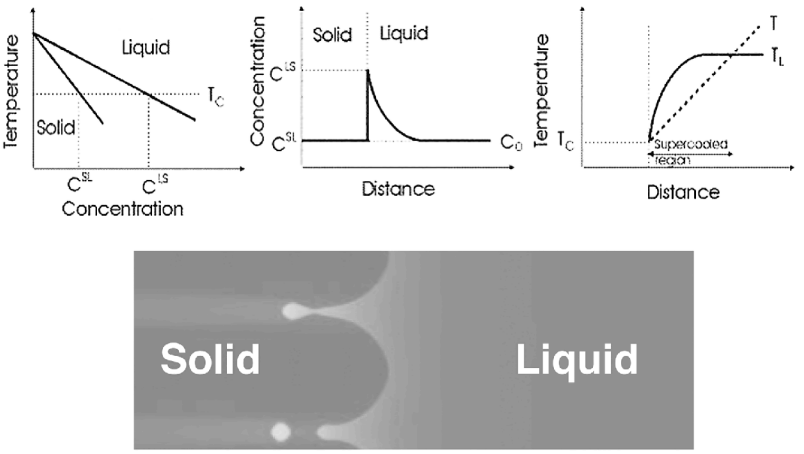


**FIGURE 6.** Above: Unstable solidification of a binary allow can arise due to constitutional supercooling. Refer to text for expalanation. Below: Cellular growth instability is computed by Bi [76] using a two-dimensional, phase field model for directional solidification of a binary alloy. The light regions show a melt enriched with one component due to solute segregation.

front of the interface. This changes with position due to the compositional profile in the melt set up by segregation and mass diffusion and the dependence of the equilibrium freezing temperature on composition, shown in the preceding plots along the top of Figure 6. Under the conditions depicted, the melt in front of the interface is below its freezing point, and a perturbation to the interface will grow rapidly into the supercooled region, resulting in a unstable growth interface. This situation is known as *constitutional supercooling,* and the criterion for it to arise is,

$$\frac{dT}{dz} < \frac{mc_0(1-k)V_g}{k\mathscr{D}}, \tag{17}$$

where $dT/dz$ denotes the axial temperature gradient of the melt at the interface and $m$ is the slope of the liquidus curve on the binary phase diagram. The resultant behavior, which is often referred to as the *Mullins–Sekerka instability* [74, 75], is a wavy interface, which, under larger driving forces, becomes successively more unstable in the form of cells and, eventually, dendrites. A phase-field computation of such an unstable interface by Bi and Sekerka [76, 77] is also shown in Figure 6.

## Process-level modeling of melt growth

Predicting the behavior of an industrial-scale melt crystal growth process requires a faithful depiction of furnace-scale heat transfer along with a detailed accounting for heat transfer, melt convection, and solid-liquid interface motion. Toward a flexible, rigorous realization of these challenges, we have developed a multi-scale, modular model to study

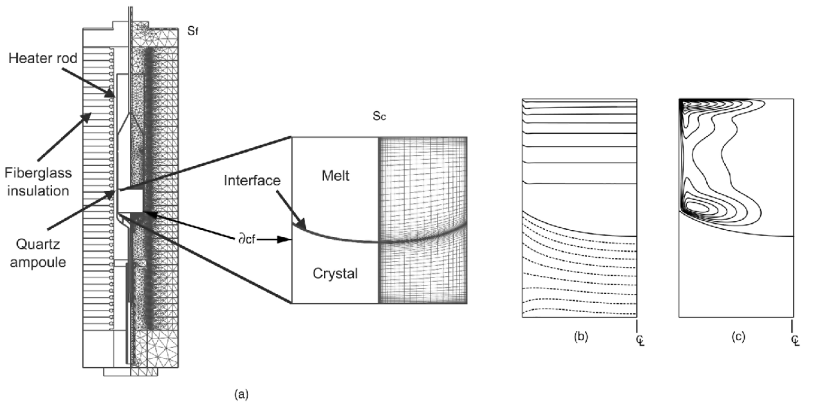


**FIGURE 7.** (a) Self-consistent model for the EDG growth of CZT, showing CrysVUn furnace model on left and Cats2D crystal growth model on right. (b) Temperature isotherms in the melt are shown by solid lines; isotherms in the crystal are dashed. (c) Melt streamlines: the flow consists of two, nested toroidal cells co-circulating in the counterclockwise direction, as viewed here. Adapted from [78].

the growth of single crystals of cadmium zinc telluride in an industrial electrodynamic gradient freeze furnace [78]. The complete model for melt crystal growth is divided into two domains, one employing the CrysVUn code [79, 80] to solve for the furnace (the *global* model), and the other employing Cats2D [81] comprising the melt, crystal, and melt-crystal interface (the *local* model). A schematic diagram is shown in Figure 7(a), where meridional views are shown of the two-dimensional, axisymmetric domains. The global model includes all of the details of the furnace and ampoule assembly, while the local model consists only of the melt, interface, and a portion of the crystal.

Sample results are shown in Figure 7 for a quasi-steady state snapshot of the system under typical operating parameters. The temperature field, depicted by isotherms in Figure 7(b), shows that the melt-crystal interface is strongly concave with respect to the solid. The dashed isotherms in the solid show a two-dimensional thermal field, with heat flowing downward and outward. Flattened isotherms in the melt with boundary layers near the ampoule wall arise due to strong convective mixing throughout most of the melt domain. Streamlines, shown in Figure 7(c), indicate flows rotating in an counterclockwise sense; the melt flow is everywhere tangent to the streamlines. Buoyant forces caused by radial thermal gradients in the bulk drive counterclockwise recirculating flows, with warmer fluid rising along the centerline and flowing downward along the walls. This flow structure is reversed compared to most Bridgman systems; however, in this extremely low-gradient system, the effect of latent heat is large enough to reverse the direction of the radial temperature gradient throughout the bulk of the melt. Surface tension gradients caused by radial thermal gradients along the melt free surface at the top of the domain lead to Marangoni forces that reinforce these recirculating flows.

While the CrysVUn-Cats2D model was able to compute a fully self-consistent solution for this multi-scale, coupled model, Pandy *et al.*[78] also demonstrated that the success of the computations depended strongly upon the details of how the two mod-

els were coupled. Indeed, convergence was only attainable under select conditions. The source of this difficulty was explained using ideas from fixed-point iterations in [82, 83]. Recent work suggests that an Approximate Block Newton method [84] is far superior than the block Gauss-Seidel algorithm used by [78].

## FINAL REMARKS

We have presented an overview of many topics relevant to the modeling of crystal growth processes, and we hope that the interested reader will further his or her knowledge via the citations presented here and in the general literature. Continuing advances in computers and algorithms are enabling increasingly powerful models for crystal growth processes. It is incumbent for any serious crystal growth practitioner to understand and utilize such tools, especially since software packages are now available for nearly all ranges of expertise and computers.

Future challenges for modeling must lead to more realistic representation of the multi-scale interactions important in crystal growth systems. Models must be capable of describing detailed system geometry and design (e.g., furnace heat transfer for melt growth systems), three-dimensional and transient continuum transport (flows, heat and mass transfer), phase-change phenomena (thermodynamics and kinetics), and atomistic events. Progress is being made on all of these fronts, but many challenges remain.

## ACKNOWLEDGMENTS

The research results shown are from projects supported in part by the Alexander von Humboldt Foundation, Department of Energy, National Aeronautics and Space Administration, National Science Foundation, and Minnesota Supercomputer Institute.

## REFERENCES

1. Douglass E. Post and Lawrence G. Votta, "Computational Science Demands a New Paradigm," *Physics Today* **58**, 35–41 (2005)
2. Karlin, Samuel, 11th R A Fisher Memorial Lecture, Royal Society 20, April 1983.
3. R.B. Bird, W.E. Stewart, and E.N. Lightfoot, *Transport Phenomena*, John Wiley, New York, 1960.
4. J.S. Szmyd and K. Suzuki, editors. *Modelling of Transport Phenomena in Crystal Growth*, volume 6 of *Developments in Heat Transfer*, WIT Press, Southampton, England, 2000.
5. J.J. Derby. "Macroscopic transport processes during the growth of single crystals from the melt," In J.P. van der Eerden and O.S.L. Bruinsma, editors, *Science and Technology of Crystal Growth*, page p. 97. Kluwer Academic Publishers, Dordecht, The Netherlands, 1995.
6. G. Müller and A. Ostrogorsky, "Convection in melt growth," In D.T.J. Hurle, editor, *Bulk Crystal Growth, Growth Mechanisms and Dynamics*, Handbook of Crystal Growth Vol. 2b, page 708. North-Holland, Amsterdam, 1994.
7. A. Yeckel and J.J. Derby, "Computational simulations of the growth of crystals from liquids," In H.J. Scheel and T. Fukuda, editors, *Crystal Growth Technology*, chapter 6. John Wiley & Sons, West Sussex, UK, 2003.
8. V. I. Polezhaev, "Modeling of technologically important hydrodynamics and heat/mass transfer processes during crystal growth," In H.J. Scheel and T. Fukuda, editors, *Crystal Growth Technology*, chapter 8. John Wiley & Sons, West Sussex, UK, 2003.

9. K. Kakimoto, "Heat and mass transfer under magnetic fields," In H.J. Scheel and T. Fukuda, editors, *Crystal Growth Technology*, chapter 7. John Wiley & Sons, West Sussex, UK, 2003.
10. C.W. Lan, "Recent progress of crystal growth modeling and growth control," *Chem. Engng. Science*, 59, 1437–1457 (2004).
11. J.J. Derby and A. Yeckel, "Modeling of Crystal Growth Processes," in: *Crystal Growth — From Fundamentals to Technology,* Eds. G. Müller, J.-J. Métois, and P. Rudolph, Elsevier, Amsterdam (2004) pp. 143–167.
12. A. Yeckel and J.J. Derby, "Computer modelling of bulk crystal growth," in: *Bulk Crystal Growth of Electronic, Optical, and Optoelectronic Materials,* Ed. P. Capper, John Wiley & Sons, West Sussex, UK, pp. 73–119 (2005).
13. J.J. Derby, "Crystal Growth: Crystal growth, bulk (Theory and Models)," in: *Encyclopedia of Condensed Matter Physics,* Eds. F. Bassani, J. Liedl, and P. Wyder, Academic Press, pp. 274–282 (2005).
14. R.A. Brown, "Theory of transport processes in single crystal growth from the melt," *AIChE J.* **34**, 881 (1988).
15. F. Dupret, J.J. Derby, K. Kakimoto, G. Müller, N. Van Den Bogaert, and A.A. Wheeler, editors, *Proceedings of the Second International Workshop on Modelling in Crystal Growth*, volume 180 of *J. Crystal Growth*. Elsevier, 1997.
16. A. Yeckel, V. Prasad, and J.J. Derby, editors, *Proceedings of the Third International Workshop on Modelling in Crystal Growth*, volume 230 of *J. Crystal Growth*. Elsevier, 2000.
17. C.W. Lan, N. Imaishi and K. Kakimoto, editors, *Proceedings of the Fourth International Workshop on Modelling in Crystal Growth*, volume 226 of *J. Crystal Growth*. Elsevier, 2004.
18. J. Friedrich and G. Müller, editors, *Proceedings of the Fifth International Workshop on Modelling in Crystal Growth*, volume 303 of *J. Crystal Growth*. Elsevier, 2007.
19. S. Brandon and J.J. Derby, "A finite element method for conduction, internal radiation, and solidification in a finite axisymmetric enclosure," *Int. J. Num. Meth. Heat Fluid Flow*, 2:299, 1992.
20. Ettouney, H.M. and Brown, R.A., "Finite element methods for steady solidification problems," *J. Computat. Phys.***49,** 118–150 (1983).
21. W. J. Boettinger, J. A. Warren, C. Beckermann, and A. Karma, "Phase-Field Simulation of Solidification," *Annual Review of Materials Research* **32**, 163-194 (2002).
22. H. Emmerich, *The Diffuse Interface Approach in Materials Science: Thermodynamic Concepts and Applications of Phase-Field Models*, Springer-Verlag, Heidelberg, 2003.
23. Winn, D. and Doherty, M. F., "Modeling Crystal Shapes of Organic Materials Grown from Solution," *AIChE J.* **46,** 1348 (2000).
24. E. van Veenendaal, A. J. Nijdam and J. van Suchtelen, "Simulation of crystal shape evolution in two dimensions," *J. Crystal Growth* **235** 603–618 (2002).
25. R.F. Sekerka, "Equilibrium and growth shapes of crystals: how do they differ and why should we care?" *Cryst. Res. Technol.* **40** 291–306 (2005).
26. Völkl J (1994) "Stress in the cooling crystal," In: Hurle DTJ (ed.) Handbook of Crystal Growth, vol. 2B, p. 821. North-Holland, Amsterdam.
27. N. Miyazaki, "Dislocation density evaluation using dislocation kinetics model," *J. Crystal Growth* **303,** 302–209 (2007)
28. T. Sinno, E. Dornberger, R. A. Brown, W. von Ammon, and F. Dupret, "Modeling and Simulation for Defect Engineering of CZ-grown Silicon Crystals," *Mater. Sci. & Eng. Rep.* **R28,** 149–198 (2000).
29. T. A. Frewen, S. S. Kapur, W. Haeckl, W. von Ammon and T. Sinno, "A Microscopically Accurate Model for Void Formation During Semiconductor Silicon Processing," *J. Crys. Growth* **279** 258–265 (2005).
30. T. Sinno, R. A. Brown, "Modeling Microdefect Formation in Czochralski Silicon," *J. Electrochem. Soc.* **146**, 2300–2312 (1999) .
31. K.A. Jackson, "Computer Modeling of Atomic Scale Crystal Growth Processes" *J. Crystal Growth* **198/199**, 1–9 (1999).
32. K.A. Jackson, "Actual Concepts of Interface Kinetics," in: *Crystal Growth — From Fundamentals to Technology* Eds. G. Müller, J.-J. Métois, and P. Rudolph, Elsevier, Amsterdam (2004) pp. 27–54.
33. G. H. Gilmer and K. A. Jackson, "Computer simulation of crystal growth," In E. Kaldis and H. J. Scheel, editors, *Crystal Growth and Materials*, page 80. North-Holland, Amsterdam, 1977.
34. J.P.J.M. van der Eerden, "Possibilities and Limitations for Numerical Simulation of Crystal Growth," in: K. Byrappa, H. Klapper, T. Ohachi and R. Fornari (eds.), Crystal Growth of Technologically

Important Electronic Materials, New Dehli: Allied Publishers PVT, Limited, 3 (2003).
35. T. Sinno, "A bottomÐup multiscale view of point-defect aggregation in silicon," *J. Crystal Growth* **303,** 5–11 (2007)
36. P. Rudolph and M. Mühlberg, "Basic problems of vertical Bridgman growth of CdTe" *Mater. Sci. Eng. B* **16,** 8–26 (1993).
37. P. Rudolph, "Fundamental studies on Bridgman growth of CdTe," *Prog. Crystal Growth and Charact.* **29,** 275–381 (1994).
38. P. Rudolph, "Non-stoichiometry related defects at the melt growth of semiconductor compound crystals – a review," *Cryst. Res. Technol.* **38**, 542–554 (2004).
39. V. M. Glazov, S. N. Chizhevskaya, and N. N. Glagoleva, *Liquid Semiconductors*, Plenum Press, New York (1969).
40. P. Rudolph, "Melt growth of II-VI compound single crystals," In M. Isshiki, editor, *Recent Development of Bulk Crystal Growth.* Research Signpost, Trivandrum, India, 1998.
41. P. Feychuk, L. Bityutskaya, E. Mashkina and L. Shcherbak, "Heat processes oscillations in the molten and solid CdTe," *J. Crystal Growth* **275**, 1827–1833 (2005).
42. V.V. Godlevsky, J.J. Derby and J.R. Chelikowsky, "*Ab Initio* Molecular Dynamics Simulations of Liquid CdTe and GaAs: Semiconducting versus Metallic Behavior," *Phys. Rev. Lett.* **81**, 4959–4962 (1998).
43. V.V. Godlevsky, M. Jain, J.J. Derby, and J.R. Chelikowsky, "First principles calculations of liquid CdTe at temperatures above and below the melting point," *Phys. Rev. B* **60**, 8640–8649 (1999).
44. J.R. Chelikowsky, J.J. Derby, V.V. Godlevsky, M. Jain, and J.Y. Raty, "Ab Initio Simulations of Liquid Semiconductors using the Pseudopotential-Density Functional Method," *J. Phys.: Condens. Matter* **13** , No 41, R817–R854, (15 October 2001).
45. M. Jain, V.V. Godlevsky, J.J. Derby, and J.R. Chelikowsky, "First principles simulations of liquid ZnTe," *Phys. Rev. B* **65**, 035212 (2002).
46. J.R. Chelikowsky, M. Jain and J.J. Derby: "Simulating Semiconductor Liquids with Ab Initio Pseudopotentials and Quantum Forces," in: *Computer Simulation Studies in Condensed Matter Physics XV,* D.P. Landau, S.P. Lewis and H.B. Schüttler (Eds.), Springer-Verlag, Heidelberg, Berlin (2002).
47. J.R. Chelikowsky, M. Jain, and J.J. Derby: "Optical Conductivity of Liquid Semiconductors" in: Computational Modeling and Simulation of Materials (Proceedings of the 10th CIMTEC World Ceramics Congress and Forum on New Materials), P. Vincenzini and A.D. Esposito (Eds.), Techna Srl. (2002).
48. W. K. Burton and N. Cabrera, "Crystal growth and surface structure: Part I," *Discussions Faraday Soc.*, **5**, 33, (1949).
49. F.C. Frank, "The influence of dislocations on crystal growth," *Discussions Faraday Soc.*, **5**, 48, (1949).
50. W. K. Burton, N. Cabrera, and F. C. Frank, "The growth of crystals and the equilibrium structure of their surfaces," *Phil. Trans. Roy. Soc. London*, **243**, 299–358, (1951).
51. A. A. Chernov, "The spiral growth of crystals," *Soviet Physics Uspekhi*, **4**, 116–148, (1961).
52. G. H. Gilmer, R. Ghez, and N. Cabrera, "An analysis of combined surface and volume diffusion processes in crystal growth," *J. Crystal Growth*, **8**, 79–93 (1971).
53. J. P. van der Eerden, "The advance velocity of steps under the influence of volume surface diffusion, by direct and indirect incorporation of growth units," *J. Crystal Growth*, **56**, 174–188 (1982).
54. H. C. Jeong and E. D. Williams, "Steps on surfaces: experiment and theory," *Surface Science Reports*, **34**, 171–294 (1999).
55. J. Krug, "Introduction to step dynamics and step instabilities," in *Multiscale Modeling in Epitaxial Growth*, A. Voigt, editor. Birkhauser, 69–96 (2005).
56. T. Michely and J. Krug, *Islands, mounds, and atoms : patterns and processes in crystal growth far from equilibrium*, Springer, Heidelberg, 2004.
57. A. A. Chernov, "How does the flow within the boundary layer influence morphological stability of a vicinal face?," *J. Crystal Growth*, **118**, 333–347 (1992).
58. A. A. Chernov, S. R. Coriell, and B. T. Murray, "Morphological stability of a vicinal face induced by step flow," *J. Crystal Growth*, **132**, 405–413 (1993).
59. S. R. Coriell, B. T. Murray, A. A. Chernov, and G. B. McFadden, "Step bunching on a vicinal face of a crystal growing in a flowing solution," *J. of Crystal Growth*, **169**, 773–785 (1996).

60. S. R. Coriell, A. A. Chernov, B. T. Murray, and G. B. McFadden, "Step bunching: generalized kinetics," *J. Crystal Growth*, **183**, 669–682 (1998).
61. A. A. Chernov, Yu. G. Kuznetsov, I. L. Smol'skii, and V. N. Rozhanskii, "Hydrodynamic effects in growth of ADP crystals from aqueous solutions in the kinetic regime," *Sov. Phys. Crystallogr.*, **31**, 705–712 (1986).
62. Y.-I. Kwon and J. J. Derby, "Modeling the coupled effects of interfacial and bulk phenomena during solution crystal growth," *J. Crystal Growth*, **230**, 328–335 (2001).
63. Y.I. Kwon, B. Dai, and J.J. Derby, "Assessing the dynamics of liquid-phase solution growth via step growth models: From BCF to FEM," *Progress in Crystal Growth and Characterization of Materials* accepted for publication (2007).
64. B. Dai, Y.-I. Kwon, and J. J. Derby, "Analysis of flow-induced, step-bunching instabilities during the growth of crystals from liquid solutions," in *Proceedings of ICTAM 2004, The XXI International Congress of Theoretical and Applied Mechanics, Warsaw, Poland*, 2004.
65. B. Dai, *Finite element modeling solution crystal growth at a meso-scale*, Ph.D. thesis, University of Minnesota, 2005.
66. M.C. Flemings, *Solidification Processing* (McGraw-Hill, New York, 1974).
67. W.A. Tiller, K.A. Jackson, J.W. Rutter, and B. Chalmers, "The redistribution of solute atoms during the solidification of metals," *Acta Metall.* **1**, 428 (1953).
68. V.G. Smith, W.A. Tiller, and J.W. Rutter, "A mathematical analysis of solute redistribution during solidification," *Can. J. Phys.* **33** 723 (1955).
69. J. A. Burton, R. C. Prim, and W. P. Slichter, "The distribution of solute in crystals grown from the melt. Part I. Theoretical," *J. Chem. Phys.*, **21**, 1987–1991 (1953).
70. E. Scheil, "Bemerkungen zur schichtkristallbildung," *Z. Mettalk.* **34**, 70–72 (1942).
71. W. R. Wilcox, "Validity of the stagnant-film approximation for mass transfer in crystal growth and dissolution," *Mat. Res. Bull.*, **4**, 265–274 (1969).
72. F. Rosenberger and G. Müller, "Interfacial transport in crystal growth, a parametric comparison of convective effects," *J. Crystal Growth*, **65**, 91–104 (1983).
73. R.A. Brown and D.H. Kim, "Modeling of directional solidification: From Scheil to detailed numerical simulation," *J. Crystal Growth*, **109**, 50–65 (1991).
74. W.W. Mullins and R.F. Sekerka, "Stability of a planar interface during solidification of a dilute binary alloy," *J. Appl. Phys.* **35**, 444 (1964).
75. R.F. Sekerka, Morphological stability, *J. Cryst. Growth* **3**, 71 (1968).
76. Z. Bi, "Directional Solidification of a Binary Alloy Using the Phase Field Model," Doctoral Thesis, Carnegie Mellon University, Pittsburgh 2001.
77. Z. Bi, R. F. Sekerka, "Phase field modeling of shallow cells during directional solidification of a binary alloy," *J. Crystal Growth* **237-239,** 138–143 (2002).
78. A. Pandy, A. Yeckel, M. Reed, C. Szeles, M. Hainke, G. Müller, and J.J. Derby, "Analysis of the growth of cadmium zinc telluride in an electrodynamic gradient freeze furnace via a self-consistent, multi-scale numerical model," *J. Crystal Growth* **276,** 133–147 (2005).
79. M. Kurz, A. Pusztai, and G. Müller, "Development of a new powerfull computer code CrysVUN++ especially designed for fast simulation of bulk crystal growth processes," *J. Crystal Growth* **198**, 101 (1999).
80. R. Backofen, M. Kurz, and G. Müller, "Process modelling of the industrial VGF crystal growth process using the software package CrysVUN++," *J. Crystal Growth* **199**, 210 (2000).
81. A. Yeckel and R. T. Goodwin, *Cats2D (Crystallization and Transport Simulator), User Manual,* Unpublished (available at http://www.msi.umn.edu/~yeckel/cats2d.html), 2003.
82. A. Yeckel, A. Pandy, and J.J. Derby, "Fixed-point convergence of modular, steady-state heat transfer models coupling multiple scales and phenomena for melt crystal growth," *Int. J. Numer. Meth. Engng.* **67,** 1768–1789 (2006).
83. J.J. Derby, L. Lun, and A. Yeckel, "Strategies for the coupling of global and local crystal growth models," *J. Crystal Growth* **303,** 114–123 (2007).
84. A. Yeckel, L. Lun, and J.J. Derby, "An efficient block-Newton algorithm for self-consistent, multiple-scale modeling of melt crystal growth," *Int. J. Numer. Meth. Engng.* submitted (2007).